XIX IMEKO World Congress
Fundamental and Applied Metrology
September 6–11, 2009, Lisbon, Portugal

CORELLATION OF NEAR AND FAR INFRARED VEIN RECOGNITION FOR UNIFIED PROCESSING AND SIMULATION.

Septimiu Crisan, Ioan Gavril Tarnovan, Bogdan Tebrean, Titus Eduard Crisan.

Department of Electrical Measurements, Faculty of Electrical Engineering, Technical University of Cluj-Napoca,
Str.C.Daicoviciu nr.15, 400020 Cluj-Napoca, Romania,
E-mail:crisans@mas.utcluj.ro

Abstract – Near infrared radiation has been successfully used in scanning vein patterns for biometric applications. While the method has been proven as highly reliable, few studies have been conducted using medium or far infrared radiation to assess the viability of a biometric scanning technique based on different wavelengths. With the constant decrease in prices for thermographic devices, the goal of this research was to determine if far infrared radiation is suitable for vein detection and to develop techniques for image processing and parameter extraction. Efforts have been made to integrate both methods (near and far infrared) in order to unify the data processing algorithms for real acquisitions and to provide enough information for performing visual reconstruction of blood vessels in simulation and database generating applications.

Keywords: vein recognition, infrared measurements, biometry

1. INTRODUCTION

Biometric recognition using vein patterns is becoming a robust technique suitable for a broad scope of applications. While the technology is not brand new, in the last years researchers have been actively studying this domain. Most of the studies relate to near infrared (NIR) scanning for different parts of the human hand [1-5] and there is a limited number of researches concerning far or long-wave infrared (LWIR) measurements [6,7].

After studying and implementing several solutions for real and simulated near infrared vein images [5,8], the focus of the authors' research has shifted towards biometric integration of multiple scanning techniques. In order to test the feasibility of a combined NIR and LWIR acquisition device, several test have been conducted using different thermographic cameras. Images of veins in the back of the hand and forearm have been acquired in controlled and uncontrolled environments and the processing algorithms used for biometric identifications of NIR images have been applied to test for possible correlations.

The results of the processed LWIR vein images have been fed to the simulation platform previously developed [8] and realistic synthetic images of far infrared human veins have been produced with minimum alterations performed on the simulation algorithms.

The paper will try to address the viability of using LWIR vein images alone and in conjunction with NIR images using roughly the same algorithm sequence. This will prove helpful for multimodal infrared vein biometrics and for the generation of large synthetic image databases of both infrared methods.

2. LWIR ACQUISITION AND PREPROCESSING

For the acquisition of LWIR vein images a small test chamber has been designed. Since the technique is based on small variations in temperature between the superficial veins and the surrounding tissue, four aspects were followed during the experiments:

- Influences of temperature on the quality of scanned images
- Modifications caused by changes in relative humidity
- Depth of veins under the skin and their overall thickness
- The degree of complexity of the model

The test chamber includes two coolers, a resistive heater and measurement devices to provide small closed-loop environmental changes.

LWIR Images from the back of the hand and the forearm have been acquired during the experiments. Two thermographic cameras have been used, a low cost device (Ti20 from FLUKE) and a high sensitivity camera, ThermaCAM B200 from FLIR.

2.1. Quality assessment for LWIR images

A method of automatically assessing the quality of the images based on a variant of the contrast coefficient previously developed in [8] has been used in order to determine the best possible scenario for image acquisition.

The images were classified (based on the method mentioned above) into five performance classes graded as follows:

ISBN 978-963-88410-0-1

- 0 – very low contrast veins, difference between average pixel values belonging to veins and background < 5
- 1 - 1ow contrast veins, difference interval [6…10]
- 2 – average contrast and clarity, difference interval [11…20]
- 3 – good contrast veins, difference interval [20…40]
- 4 – excellent contrast between veins and the surrounding tissue, difference interval [40…100]

Based on the results obtained from the NIR method, the appropriate test subjects were scanned. The set of images contained data from people with hard to see veins, thick blood vessels or circulatory problems. For subjects having thin veins for examples, all the other parameters (complexity of the vein model, depth of veins etc.) were average so that there are very few cross-results.

Table 1. Image classification based on clarity and contrast.

Vein model type	**Test chamber temperature (°C)**			
	22	**25**	**28**	**31**
Surface veins	3	3	2	1
Deep veins (invisible)	2	1	1	0
Circulatory problems	2	1	0	0
Complex vein model	3	3	1	1
Thin veins	1	1	0	0
Thick veins	4	3	3	2
Average model low humidity	3	2	2	1
Average model high humidity	2	1	1	0

As described in Table 1, best results were obtained at low temperature and low humidity thus improving the contrast. The resolution and spectral sensibility of the camera pays a significant role since for close veins or thin veins the temperature differences were almost to small to quantify.

2.2. Image preprocessing

A normal scanned LWIR image of the back of the hand displayed in greyscale is shown in Fig. 1.

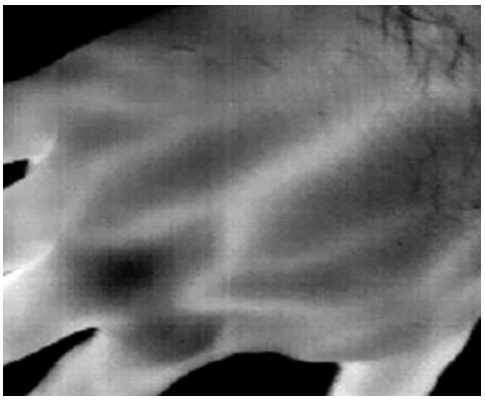

Fig. 1. Example of an average LWIR image scan (displayed in greyscale).

The span and level of the thermographic cameras were managed automatically while keeping background interference to a minimum. Also, the hand position was not constrained for images acquired by the system.

A false colour representation of a subject's forearm is depicted in Fig. 2. The contrast has been enhanced by using a restrictive colour palette.

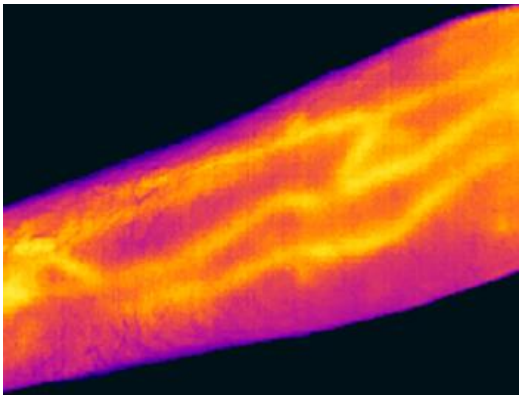

Fig. 2. LWIR Forearm visualisation in false colours with restrictive colour palette.

The image output has been confined to 320 pixels over 240 pixels and the preferred bit depth was 8. Using these restrictions, no modifications had to be made to the processing algorithm chain employed in scanning near infrared images.

3. ALGORITHM CORELLATION FOR BIOMETRIC INTEGRATION

When processing NIR images the raw picture has a whiter tissue background with almost black veins that can be easily processed as depicted in Fig. 3.

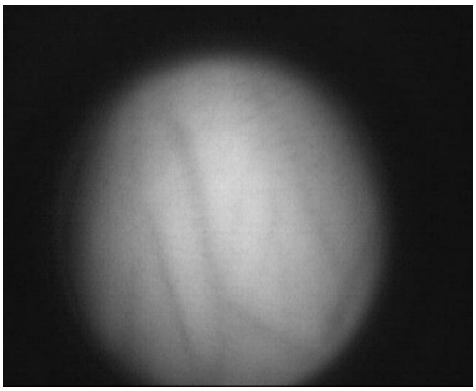

Fig. 3. Near infrared scanned image of the veins in the back of the hand.

For far infrared vein images, the situation is reversed because veins have higher temperature and therefore will appear lighter on a conventional colour palette. Since the background (area around the hand) is black on both methods it can be easily subtracted. By applying a histogram computation, the system can detect if it is processing NIR or LWIR images.

The four classes of images catalogued using the automatic contrast variation tool were tested with the NIR image processing algorithm. The fifth class was not used since there were only few images that had enough quality to belong to that level and were considered exceptions. However, this class was used as a standard for comparison between images.

The algorithm sequence is similar, since, after determining the nature of the raw image, the same operations are applied:

- Background removal
- Vein pattern centering
- Mean filter with a 3x3 kernel
- Selective contrasting
- Locally adaptive thresholding with variable overlapping kernel sizes [3x3…11x11]
- Median filter with a 5x5 kernel (2 passes for each image)
- Erosion and branch pruning
- Simplified rotation invariant 15 rule model thinning with diagonal reduction
- Pattern optimisation
- Feature extraction (nodes, terminations, intersection angles, number of segments and total segment length)

An image flag is attached to differentiate between the types of image. This procedure is necessary because the segmentation technique used in the processing algorithm will require a different number of steps and larger kernel sizes for LWIR images.

Because it is a thermal method, far infrared scanning exacerbates the thickness of the veins since heat radiates from the actual blood vessel to the surrounding tissue. This is shown in Fig. 4 where a Class 4 LWIR diffused image is segmented.

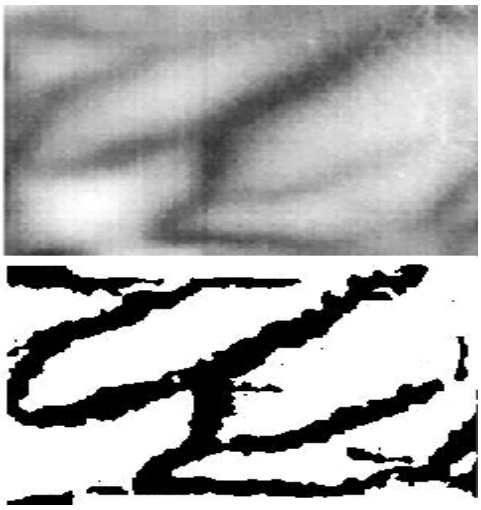

Fig. 4. Adaptive thresholding applied to a LWIR vein model image showing increased thickness.

Another important difference is related to the pruning algorithm. Extraneous branches are sometimes created by the thinning method because of the inconsistency of the image contrast throughout the scanned picture. The length of the pruned branches is higher in LWIR images.

The tests show that images belonging to Class 0 and Class 1 are very difficult to process because of the small temperature differences between the veins and the tissue. In this case the chance of detecting false key points greatly increases. This shows that the error rates are greatly influenced by the environment where the images are scanned. Class 2 images will yield good results with small alterations to the image processing algorithm. Because of this, for every image presented to the system, the image class is determined on the spot and appropriate measures are taken to change the number of steps for each processing operation.

For a given matching score, the system is able to recognize all entries belonging to Class 3 and Class 4 images. The matching score is based on (1).

$$S_s = 100 - \left[\text{int}\left(\frac{\left(1 - \frac{N_{p1}}{N_{p2}}\right)}{3} \right) + 5\left(\left|N_{S1} - N_{S2}\right|\right) + 7\left(\left|N_{T1} - N_{T2}\right|\right) + \text{int}\left(\frac{\left(1 - \frac{D_{T1}}{D_{T2}}\right)}{2} \right) \right] \quad (1)$$

where:

N_{P1}, N_{P2} are the total number of pixels for the two thinned images (comparison and experiment)

Ns_1, Ns_2 represent the number of segments from the two images

N_{T1}, N_{T2} are nodes and terminations for the images

D_{T1}, D_{T2} are distances between nodes and terminations in both images

In the case of Class 2 images, the best matching score yields a FAR (false accept rate) equal to 0.026% and the FRR (false rejection rate) is 1.08% for a database size of 206 real and 4400 simulated images. Class 1 and Class 0 are unusable due to the high error rates.

The vein simulation platform VEINSIM has been updated to include realistic representations of LWIR vein images.

4. CONCLUSIONS

The paper has presented an analysis of LWIR vein images to test their use for biometric scanning. The LWIRst tests are encouraging since controlled environments with cooler temperature can produce high enough contrast. The algorithms used for image processing were the same as those being employed in NIR vein scanning with small variations (number of steps, kernel sizes etc). The class differentiation between images helps selecting the best course of action for biometric feature extraction.

Using this method, a single system can be built to analyze NIR and LWIR vein structure data. With the decrease in thermal vision camera prices, it will soon be possible to integrate both technologies into a multimodal scanning device with added liveness detection security due to the temperature being scanned.

The analysis of LWIR images has also led to the improvement of VEINSIM that can allow the creation of accurate synthetic images of hands scanned with far infrared radiation

REFERENCES

[1] Badawi, A. M. "*Hand Vein Biometric Verification Prototype: A Testing Performance and Patterns Similarity"*. Proceedings of the 2006 International Conference on Image Processing, Computer Vision, and Pattern Recognition, Las Vegas USA

[2] Miura, N., Nagasaka, A. şi Miyatake, T. *"Personal identification device and method"*. Hitachi, Ltd., US Patent 6993160, 2006

[3] *** Vein pattern recognition www.fujitsu.com

[4] Nadort, Annemarie, "*The hand vein pattern used as a biometric feature*", Nederlands Forensisch Instituut, May 2007

[5] Septimiu Crisan, I.G. Târnovan, T.E.Crisan, *„Vein pattern recognition. Image enhancement and feature extraction algorithms",* 15th IMEKO TC4 Symposium, Iaşi, Romania, 2007, ISBN 978-973-667-260-6

[6] Lin, C.-L. şi Fan, K.-C., *"Biometric Verification Using Thermal Images of Palm-Dorsa Vein Patterns*". IEEE Transactions on ciruits and systems for video technology 14, pp 199 – 213, 2004

[7] Smith, C. L. şi Cross, J. M. "Thermographic imaging of the subcutaneous vascular network of the back of the hand for biometric identification". *Security and Technology Proceedings. Institute of Electrical and Electronics Engineers 29th Annual International Carnahan Conference on*, pp 20-35, 1995

[8] Septimiu Crisan, I.G. Târnovan, T.E.Crisan, *„ A hand vein structure simulation platform for algorithm testing and biometric identification",* 16th IMEKO TC4 Symposium, Florence, Italy, sept. 2008

[9] Gray, Henry. "Anatomy of the Human Body". Philadelphia: Lea & Febiger, 1918; Online edition Bartleby.com, May 2000.

[10] *** Finger vein scan technology, www.hitachi.com

[11] Dragomir, N.D., et. al.. - *Măsurarea electrică a mărimilor neelectrice*, Vol 2, Ed.Mediamira Cluj-Napoca, 1998

[12] *** The Biometric Consortium "*Introduction to Biometrics", 2002*

[13] Jain A.K., Bolle R. & Pankanti S. "*Biometrics: Personal Identification in Networked Society"* Kluwer Academic Publishers, 1999

[14] A. D. Kim, *"Transport theory for light propagation in biological tissue,"* Optical Society of America Journal A 21, pp. 820–827, May 2004.